ARTICLES

Constructing a Tunable Chemical Oscillator

Fernando Montoya[†] **and P. Parmananda***[,†,‡]

Facultad de Ciencias, UAEM, Avenida Universidad 1001, Colonia Chamilpa, C.P. 62209, Cuernavaca, Morelos, México, and Department of Physics, Indian Institute of Technology Bombay, Powai, Mumbai 400076, India

Received: October 20, 2008; Revised Manuscript Received: December 23, 2008

The possibility of designing a tunable chemical oscillator is explored. In contrast to a normal oscillator which when subjected to external forcing exhibits the characteristic unimodal resonance curve, a tunable oscillator reveals a constant response curve. This persistence of resonant behavior for a wide interval of forcing frequencies is seeked both numerically and in an experimental electrochemical cell. Our results indicate that, although challenging, a tunable chemical oscillator can indeed be conceived.

1. Introduction

Periodic forcing of oscillating systems has been exhaustively investigated in diverse electrical,[1,2] chemical,[3,4] and biological[5] systems. As a consequence of the underlying entrainment phenomena these forced systems exhibit a variety of different dynamical responses such as periodic, quasi-periodic, and chaotic behavior. Another aspect of periodically forced self-oscillating systems, which in comparison has received much less attention, involves the generation of multiple coexisting attractors (multistability)[6,7] for an appropriate perturbing function. It is widely accepted that most of the results for forced oscillating systems remain valid for oscillators operating in the fixed point regime, for example, exhibiting excitable fixed point behavior.[8] The only requirement is that the superimposed forcing be superthreshold thereby ensuring that the oscillatory domain is frequently visited.

Simpler dynamics are observed for the scenario wherein the external forcing is subthreshold. For an overdamped oscillator (dynamics exhibiting stable node behavior), the system response decreases monotonically as the forcing frequency is augmented. In contrast, scanning the perturbation frequency (maintaining amplitude constant) invokes the classical resonance curve for an underdamped oscillator (dynamics exhibiting stable focus behavior). The peak of this unimodal curve (maximal response) occurs for the resonant frequency. The possibility of designing an oscillator that would be able to exhibit maximal response not just for one frequency but for a wide interval of forcing frequencies is rather enticing. It would entail the construction of an oscillator which could be tuned in accordance to the frequency of the superimposed perturbation. Apart from being an interesting and challenging scientific problem, designing of such an oscillator might have some correspondence to the functioning of the human auditory system. It is well-known that the human ear detects signals in the audible range (20−20000 Hz) with commensurable efficiency. Although the underlying nature of the auditory system is extremely intricate and involves complex biochemical processes, there have been some reports[9,10] claiming that auditory sensitivity is provided by the self-tuned critical oscillations of hair cells in the inner ear. Previous endeavors involving the configuration of tunable oscillators have involved vibrating soap films[11] and vibrating strings with freely sliding metal beads.[12] Adaption in these systems occurs naturally (self-adaptive) due to the inherent properties of the system, namely, the availability of an extra (free) degree of freedom. In stark contrast to these previous works, in the present contribution we entertain the possibility of devising a tunable chemical oscillator which does not possess a free internal degree of freedom and therefore normally would not exhibit adaptive behavior. Numerical simulations, using a corrosion model, were carried out as a precursor to subsequent experimental endeavors employing an electrochemical cell.

2. Simulation Results

To design a tunable oscillator numerically, the following corrosion/passivation model described by two dimensionless coupled nonlinear differential equations is used

$$\dot{Y} = p(1 - \theta_{OH}) - qY \tag{1}$$

$$\dot{\theta}_{OH} = Y(1 - \theta_{OH}) - [\exp(-\beta\theta_{OH})]\theta_{OH} \tag{2}$$

The two variables θ_{OH} and Y represent the fractional coverage of the electrode surface covered by a passivating metal hydroxide film and the concentration of metal ions in the electrolytic solution, respectively. The kinetic rate constants of the governing chemical reactions determine the values for the system parameters p, q, and β. Prior numerical studies[13,14] indicate that this model system exhibits stable focus dynamics for appropriate parameter values. The model equations are numerically integrated using a fourth-order Runge−Kutta algorithm with a constant step size of $h = 1$. The sinusoidal modulation, $p(t) = p_0(1 + A \sin(\omega t))$ where $p_0 = 1.31 \times 10^{-4}$, of the system parameter p represents the superimposed external forcing. Figure 1a shows the stable focus behavior of the autonomous system whereas in Figure 1b the resonance curve

* Corresponding author.
† Facultad de Ciencias, UAEM.
‡ Department of Physics, Indian Institute of Technology Bombay.

10.1021/jp809281z CCC: $40.75
Published on Web 01/30/2009

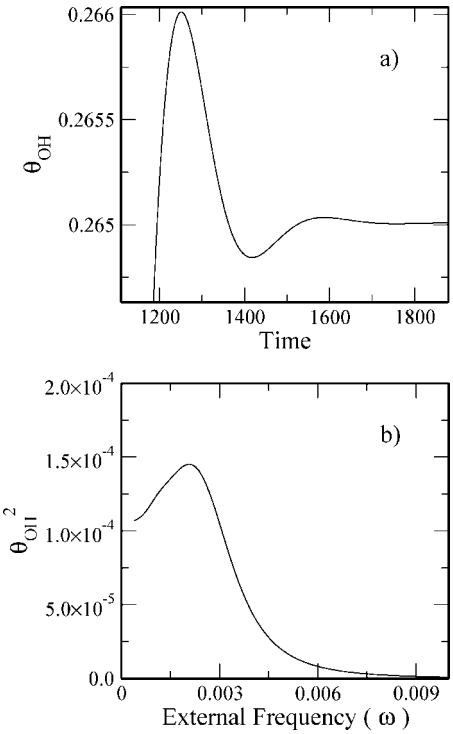

Figure 1. The numerical dynamics for the corrosion/passivation model. The model parameters are chosen, $\{p, q, \beta\} = \{1.31 \times 10^{-4}, 1.0 \times 10^{-3}, 5.0\}$, such that the autonomous dynamics exhibit a stable focus behavior. All the plotted quantities are dimensionless. (a) The dissipative under damped dynamics in the vicinity of the stable focus fixed point. (b) The resonance curve obtained when the model parameter p is modulated sinusoidally $p = p_0(1 + A \sin(\omega t))$ where $p_0 = 1.31 \times 10^{-4}$. A, the forcing amplitude, is kept constant at $A = 1 \times 10^{-6}$ whereas ω, the forcing frequency, is varied. The quantity θ_{OH}^2, plotted in the resonance curve of Figure 1b is the square of the oscillation amplitude for the model variable θ_{OH}.

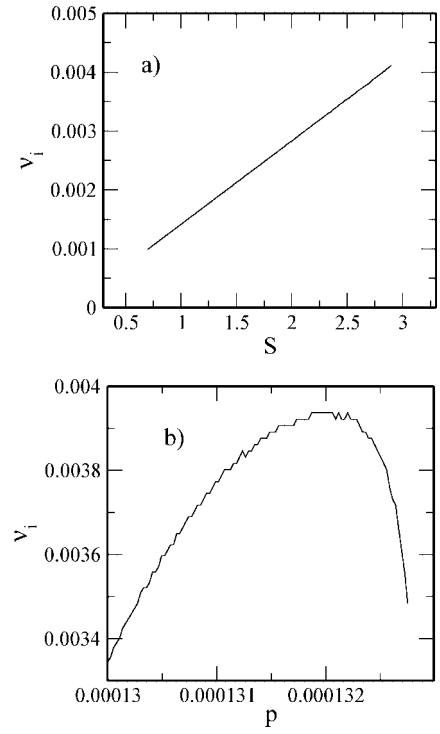

Figure 2. The variation of the intrinsic frequency ν_i as a function of the two appropriate model parameters S and p. All the plotted quantities are dimensionless. (a) The linear variation of the intrinsic frequency ν_i as a function of the model speed S. The other model parameters are maintained constant $\{p, q, \beta\} = \{1.31 \times 10^{-4}, 1.0 \times 10^{-3}, 5.0\}$. (b) The variation of the intrinsic frequency ν_i as a function of the bifurcation parameter p. The other parameters $\{S, q, \beta\} = \{2.5, 1.0 \times 10^{-3}, 5.0\}$ remain constant.

for the forced system is presented. The model and the forcing parameters are provided in the corresponding figure caption.

In order to achieve tuning numerically, model parameters that change the intrinsic frequency ν_i of the model dynamics need to be identified. Thereafter, as the frequency ν_e of the external forcing is varied, these model parameters need to adjust appropriately such that the condition $\nu_i = \nu_e$ is constantly satisfied. The first obvious numerical parameter that changes ν_i is the model speed S. Multiplying the right-hand sides of eq 1 and eq 2 with a constant factor (S) alters the frequency (ν_i) of the dissipative dynamics in the vicinity of the stable focus. Figure 2a shows the expected linear variation of ν_i as a function of the S. The bifurcation/control parameter p also modifies the intrinsic frequency of the model dynamics as shown in Figure 2b. Subsequently, using linear approximation, if necessary, ($\Delta\nu_i/\Delta S$) and ($\Delta\nu_i/\Delta p$) need to be computed for the two curves. Evidently, in Figure 2b this would restrict the frequency interval for which tuning could be attained. In the case of parameter S, the relation $\nu_i(S) = 0.0014169S$ is derived using the curve of Figure 2a. Inverting this previous equation and using the tuning condition ($\nu_i = \nu_e$) yields $S(\nu_e) = 705.766\nu_e$, the functional form for the tuning parameter S that ensures adaptation. An identical analysis for the parameter p (Figure 2b) gives $\nu_i(p) = (353.74p + 0.0033963)$ which subsequent to appropriate inversion reveals $p(\nu_e) = (\nu_e - 0.0033963)/353.74$ as the seemingly adequate variation for the tuning parameter p to achieve tunability.

Figure 3 shows the numerical results involving tuning behavior in the corrosion model. The successful adaptation in the forced oscillator is exemplified by the persistence of the maximal response for a range of values of ν_e. Correspondingly, the characteristic unimodal resonance curve is replaced by a constant response. Although the tuning using parameter S directly yields the straight line response presented in Figure 3a, the resonance curve presented in Figure 3c, using parameter p, can only be calculated subsequent to a suitable scaling procedure for the following reason: Increasing the bifurcation parameter p the system dynamics evolve from a stable node behavior (over damped), to a stable focus behavior (under damped) and eventually nearing the supercritical Hopf bifurcation point. Accordingly, as shown in Figure 3b, the maxima of the provoked resonance curve increases as the parameter p approaches the Hopf bifurcation point. Therefore, varying the parameter p changes not only the intrinsic frequency (ν_i) of the system but also the maximum attainable amplitude. As a result, even in the case of successful adaptation, the absolute value of the maximum provoked response would not maintain constant. However, if one appropriately scales the response amplitudes (in comparison to the maxima of the corresponding resonance curve) for different forcing frequencies, a reasonable adaptation can be achieved, as shown in Figure 3c.

3. Experimental Results

The next stage of the present work involves designing a tunable oscillator experimentally in a three-electrode electrochemical cell. This system is related to the electrochemical model discussed before since the underlying chemical processes in both cases involve the electrochemical corrosion (electrodissolution) of the metal surface in an aqueous media. Therefore, the generic electrodissolution model captures qualitatively some of the dynamical behavior observed experimentally.

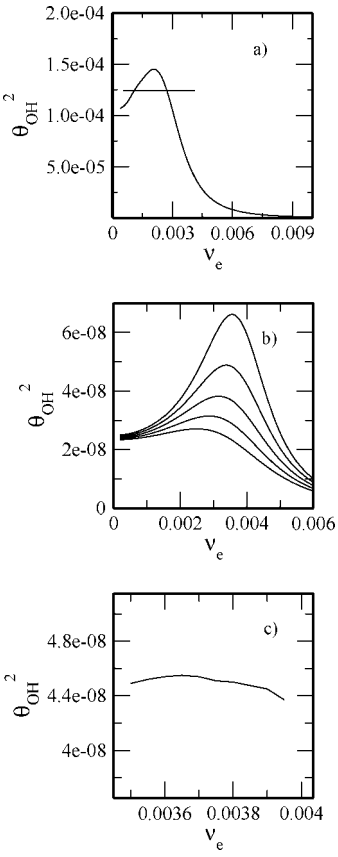

Figure 3. Numerical results indicating attainment of tunable behavior using the protocol involving linearization and inverting functions as explained in the text. All the plotted quantities are dimensionless. (a) The resonance curves without (unimodal) and with (straight line) adaptation using the speed parameter S. (b) The different resonance curves provoked using the parametric forcing $p = p_0(1 + A \sin(\omega t))$ for five values of p_0 (1.3015×10^{-4}, 1.3045×10^{-4}, 1.3075×10^{-4}, 1.3105×10^{-4}, 1.3135×10^{-4}). The maximal attainable amplitude augments as p_0 is increased since the system progresses from the overdamped → underdamped dynamics eventually approaching the Hopf bifurcation. The other model parameters $\{S, q, \beta\} = \{2.5, 1.0 \times 10^{-3}, 5.0\}$ remain constant. (c) Resonance curve (subsequent to a suitable scaling) indicating the tunable behavior using the bifurcation parameter p.

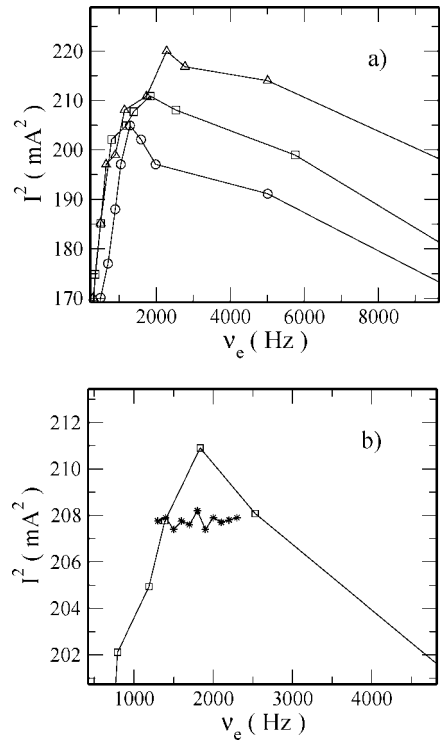

Figure 4. Experimental results indicating attainment of adaptation of the anodic current (I (mA)) using the tuning protocol involving linearization and function inverting as described in the text. (a) Three of the seven experimental resonance curves computed to calculate $(\Delta\nu_i)/(\Delta V)$. The ones presented correspond to anodic voltages of 600 mV (circles), 750 mV (squares), and 900 mV (triangles), respectively. (b) The resonance curves without (unimodal) and with (asterisk) tuning using the experimental bifurcation parameter V. The quantity I^2 plotted in the resonance curve is the square of the oscillation amplitude for I, the experimental variable. The parameter $V = V_0(1 + A \sin(2\pi\nu t))$ is modulated continuously with $V_0 = 750$ mV and $A = 60$ mV. It is remarkable that adaptation can persist for a frequency interval of about 1000 Hz.

The anode and cathode of this cell are identical carbon steel disk (7 mm diameter) electrodes shrouded by epoxy, whereas the reference is the saturated calomel electrode (SCE). These three electrodes are immersed in a sodium chloride NaCl solution 10% in weight, and a volume of 500 mL is maintained in the electrochemical cell.[15−17] The experiments are carried out potentiostatically such that the anodic potential (V) between the anode and reference is maintained constant whereas the anodic current (I) between the anode and cathode is recorded for analysis. This experimental configuration is of extreme industrial relevance and has been used before to replicate the corrosion environment of carbon steel, the material commonly employed in the construction of pipelines used to transport seawater (hydrocarbons). Previous studies[17] indicate that the interval of anodic voltage -900 mV $< V_0 < -600$ mV is of interest for the present experiments.

Experimental resonance curves are generated via periodic modulations of the anodic voltage ($V = V_0(1 + A \sin(2\pi\nu_p t))$. Figure 4a shows three of the seven experimental resonance curves calculated for different anodic voltages (V_0). In contrast to the numerical curves presented in Figure 3b where varying the control parameter (p) changed the intrinsic frequency as well as the provoked amplitude, the experimental curves (Figure 4a) indicate that the maximal provoked amplitude essentially remains unchanged. Similar to the numerical calculations, a linear function $\nu_i(V) = 10(V - 210)/3$ Hz is obtained. Inverting the functional form in conjunction with the tunability condition ($\nu_i = \nu_e$) divulges the voltage variation, $V(\nu_e) = 0.3(\nu_e) + 210$ mV, that should achieve a constant resonance curve. In this tunability condition, the constants 0.3 (slope) and 210 mV (intercept) are inherent to the electrochemical cell and are a measure of the response/stimulus factor of the experimental system when subjected to external forcing. Moreover, this tunability condition remains valid in the parameter interval where the autonomous systems exhibits underdamped dynamics (stable focus behavior) in the vicinity of the Hopf bifurcation. Figure 4b shows the experimental resonance curves with and without tuning. The almost straight line with experimental data points (represented by asterisks) divulges the persistence of a constant system response for an external frequency interval of about 1000 Hz.

4. Discussion

The numerical parameter p and the experimental parameter V used to achieve tuning are comparable. An analogous to the numerical parameter S in the experimental chemical system could be temperature which, in our experiments, did increase the frequency of the oscillations. Unfortunately, we did not have

the necessary infrastructure to attempt tuning with temperature in our electrochemical cell.

To summarize, a tunable oscillator was constructed both numerically and experimentally. Although the present results involve adaptation in an electrochemical system, the tuning method is general and therefore valid for all classes of nonlinear oscillators. The two necessary conditions for the implementation of this tuning protocol are as follows: (a) The nonlinear system exhibits underdamped dynamics (stable focus behavior). (b) There exists an accessible system parameter which can vary the intrinsic frequency of the nonlinear system. We were also able to construct a tunable oscillator for the FitzHugh−Nagumo model system wherein the dynamics are inherently excitable (results not shown). This points to the applicability of our tuning protocol to different types of autonomous behavior. This method, in actual experiments, could also be used for detecting the location of Hopf bifurcations in the parameter space. The increase in the maximal response amplitude of the tuned system would be an indication that the autonomous dynamics is approaching the bifurcation point.

Previous works in this direction involved special systems such as vibrating strings and soap films which were able to self-adapt due to an internal degree of freedom. However the majority of the real systems do not possess this extra degree of freedom and consequently cannot exhibit self-adaptation. Our method could enable such systems to tune with external forcing.

Acknowledgment. F.M. and P.P. acknowledge financial support from CONACyT through Grant No. 40885/A1 and Grant No. 48354-F, respectively.

References and Notes

(1) Yeh, W. J.; He, D. R.; Kao, Y. H. *Phys. Rev. Lett.* **1984**, *52*, 480.
(2) Martin, S.; Martienssen, W. *Phys. Rev. Lett.* **1986**, *56*, 1522.
(3) Buchholtz, F.; Schneider, F. W. *J. Am. Chem. Soc.* **1983**, *105*, 7540.
(4) Eiswirth, M.; Ertl, G. *Phys. Rev. Lett.* **1988**, *60*, 1526.
(5) Aihara, K.; Matsumoto, G.; Ikegaya, Y. J. *Theor. Biol.* **1984**, *109*, 249.
(6) Rehmus, P.; Vance, W.; Ross, J. *J. Chem. Phys.* **1984**, *80*, 3373.
(7) Rivera, M.; Parmananda, P.; Eiswirth, M. *Phys. Rev. E* **2002**, *65*, 025201.
(8) Dolnik, M. M.; Padusakaa, E.; Marek, M. *J. Phys. Chem.* **1987**, *90*, 4407.
(9) Camelet, S.; Duke, T.; Jülicher, F.; Prost, J. *Proc. Natl. Acad. Sci. U.S.A.* **2000**, *97* (7), 3183.
(10) Jülicher, F.; Andor, D.; Duke, T. *Proc. Natl. Acad. Sci. U.S.A.* **2001**, *98* (16), 9080.
(11) Boudaoud, A.; Couder, Y.; Ben Amar, M. *Phys. Rev. Lett.* **1999**, *82*, 3847.
(12) Boudaoud, A.; Couder, Y.; Ben Amar, M. *Eur. Phys. J. B* **1999**, *9*, 159.
(13) Talbot, J. B.; Oriani, R. A. *Electrochim. Acta* **1985**, *30*, 1277.
(14) Markworth, A. J.; McCoy, J. K.; Rollins, R. W.; Parmananda, P. In *Applied Chaos*; Kim, J. H., Stringer, J., Eds.; John Wiley & Sons, Inc.: New York, 1992.
(15) Bertocci, U. *Corrosion* **1979**, *35*, 211.
(16) Lalvani, S. B.; Zhang, G. *Corros. Sci.* **1995**, *37*, 1571.
(17) Rivera, M.; Uruchurtu-Chavarín, J.; Parmananda, P. *Phys. Rev. Lett.* **2003**, *90*, 174102.

JP809281Z